**Agnieszka LENART[*], Paweł PAWLUS[**], Andrzej DZIERWA[**], Mirosław TUPAJ[**]**

# THE EFFECT OF SURFACE TEXTURE OF STEEL DISC ON FRICTION AND FRETTING WEAR

## WPŁYW STRUKTURY GEOMETRYCZNEJ POWIERZCHNI TARCZ STALOWYCH NA TARCIE I ZUŻYCIE FRETTINGOWE

**Key words:** surface topography, friction, wear.

**Abstract** Fretting tests were performed using an Optimol SRV5 tribotester in a ball-on-flat scheme. Balls from 100Cr6 steel of 60 HRC hardness and diameters of 10 mm co-acted with discs from 42CrMo4 steel of 47 HRC hardness under dry gross fretting conditions. Tests were performed at 30$^0$C and 25–35% relative humidity, and the number of cycles was 18000. During each test, the normal load was kept constant. Six sets of experiments were conducted. Discs had different surface textures as the result of machining. It was found that the lowest coefficients of friction were obtained for anisotropic surfaces when ball movements were perpendicular to main disc texture directions.

**Słowa kluczowe:** topografia powierzchni, tarcie, zużycie.

**Streszczenie** W badaniach zastosowano tester tribologiczny Optimol SRV5. Kulka ze stali 100Cr6 o twardości 60 HRC kontaktowała się z tarczą o średnicy 10 mm wykonaną ze stali 42CrMo4 o twardości 47 HRC w warunkach frettingu. Temperatura wynosiła 30°C, wilgotność względna 25–35% przy liczbie cykli równej 18000. Tarcze charakteryzowały się zróżnicowaną strukturą geometryczną powierzchni uzyskaną w wyniku obróbki. Najmniejsze współczynniki tarcia osiągnięto, kiedy ruch kulki odbywał się prostopadle do głównego kierunku ukształtowania powierzchni tarczy.

## INTRODUCTION

Fretting is a relative motion with a small amplitude between two oscillating surfaces. When the sliding amplitude is smaller than a Hertzian contact radius, reciprocating sliding occurs **[L. 1]**. Depending on the relative displacements and the normal load, different sliding regimes can be identified: stick, partial slip, and gross slip **[L. 2, 3]**. Varenberg et al. **[L. 4, 5]** introduced criterion, named the *slip index* to define the fretting regime on the basis of the fretting loop. For small displacement amplitudes, the contact displays composite structure of sticking and sliding areas (partial slip). For higher amplitudes, the entire contact is subjected to sliding (gross slip) **[L. 6]**. Fretting damage mode depends on sliding regimes, leading to cracking under partial slip and wear under gross slip conditions. Fretting wear combines various basic wear mechanisms: adhesion, abrasion, surface fatigue, and oxidation **[L. 7]**.

In fretting wear, the generated oxide debris, trapped at surfaces and providing a load-carrying plateau, is of importance. Two opposite effects of wear particles on material loss were identified, which are beneficial due to formation of the oxide layer and harmful due to the abrasive action of debris **[L. 9]**. Varenberg et al. **[L. 7]** found that, for adhesive wear, debris reduced and for abrasive wear facilitated damages. Wear particles can also affect the coefficient of friction **[L. 10]**. The authors of Reference **[L. 11]** studied fretting wear behaviour of a SiC reinforced aluminium matrix composite against a carbon steel. Wear particles increased in size with increased fretting stroke. For fretting of steel, the abrasive particles formed in air are loose and non-cohesive; they can be easily eliminated **[L. 12]**.

[*] Heli-One, 36-102 Jasionka 947, Poland.
[**] Rzeszow University of Technology, Faculty of Mechanical Engineering and Aeronautics, Powstańców Warszawy 8, 35-959 Rzeszow, Poland.

Previous research reported in **[L. 13]** suggested that there are about 50 variables affecting the fretting wear process, including amplitude of displacement, contact pressure, frequency, and surface hardness. Under a gross slip regime, wear increased when displacement amplitude increased **[L. 14, 15]**. Toth **[L. 16]** found that fretting wear of steel samples was reduced with increasing frequency, and the frequencies were between 0.01 and 60 Hz. Soderberg et al. **[L. 17]** conducted fretting experiments for steel counterparts in the frequency range from 10 to 10000 Hz.

The relationship between fretting wear and hardness is complex. Kayanba and Iwabuchi **[L. 18]** found that harder steel wore more than softer steel, due to protection of the harder surface by an oxide debris layer. A structural steel with different hardness was fretted against bearing steel with constant hardness **[L. 19]**. Variation in wear rate with the hardness of the structural steel was not observed. Budinsky **[L. 20]** performed fretting tests with hard steel against different steels that had various hardnesses. He found that the overall wear rate increased for a significant difference between the hardness of two mating parts. Lemm et al. **[L. 21]** employed the same steel for both parts of the fretting assembly, with the hardness of both samples being varied after heat treatment. When the difference between the hardness of the two specimens exceeded a critical value, a harder specimen wore much than a softer.

The surface preparations are essential to monitor and reduce damage caused by fretting; however, effects of surface topography are often neglected. But surface roughness seems to have large impact on the presence of wear particles in the contact area. However, the results of the experimental investigation of roughness effect on fretting are sometimes contradictory. Kubiak et al. **[L. 22, 23]** achieved a smaller coefficient of friction for rougher disc textures. Pawlus et al. **[L. 24]** found that, for rougher disc topographies, the friction force and wear of the system were larger. The influence of sphere surface roughness on fretting in a gross slip regime was studied experimentally by Yoon et al **[L. 25]**.

As can be seen from the literature review, the influences of surface roughness on fretting are still disputable and sometimes contradictory. It is difficult to find in the open literature research analysing the influence of surface texture on fretting in various operating regimes. The work described in this paper tries to fill this gap.

## EXPERIMENTAL DETAILS

Fretting tests were performed using an Optimol SRV5 tribotester in a ball-on-flat configuration. Steel 100Cr6 balls of 60 HRC hardness and diameters of 10 mm co-acted with 42CrMo4 steel of 47 HRC hardness under dry gross fretting conditions (the criteria from papers **[L. 1, 4, 5]** were fulfilled). Tests were performed at $30^0$C and 25–35% relative humidity, and the number of cycles was 18000. During each test, the normal load was kept constant. For each type of tests, six sets of experiments were conducted, and **Table 1** lists operating conditions for various types of tests. Before the tests, specimens were cleaned in acetone.

Machined and worn surface topographies of discs and balls were measured using a Talysurf CCI Lite white light interferometer. The areas of 3.3 x 3.3 mm$^2$ contained 1024 x 1024 points. The roughness of the balls determined by the Ra parameter was 0.15 μm. The discs had different surface topographies resulting from polishing (P), lapping (L), milling (M), grinding (G), and vapour blasting (VB) techniques. Friction tests of anisotropic disc textures after milling and grinding were performed orthogonally to the lay (main surface direction). The total net volume $V_{tot}$ of tribological system was calculated as follows:

$$V_{tot} = V_{disc} + V_{ball},$$

$$V_{disc} = (V_{disc}\text{-}) - (V_{disc}+),$$

$$V_{ball} = (V_{ball}\text{-}) - (V_{ball}+),$$

where positive volumes,, ($V_{disc}$+) and ($V_{ball}$+), were considered as transferred materials or build up, while negative volumes, ($V_{disc}^-$) and ($V_{ball}^-$), as lost material

**Table 1. Conditions of fretting tests**
Tabela 1. Warunki testów

| Test designation | Disc hardness, HRC | Amplitude A, mm | Frequency f, Hz | Normal force P, N | Disc samples |
|---|---|---|---|---|---|
| IA | 47 | 0.1 | 20 | 45 | VBI1, VBI2, MI1, MI2, MI3, GI1, GI2, PI, LI |
| IB | | 0.075 | 20 | 45 | |
| IC | | 0.05 | 20 | 45 | |
| ID | | 0.05 | 20 | 15 | |
| IE | | 0.05 | 50 | 15 | |
| IF | | 0.05 | 50 | 45 | |
| IIF | | 0.05 | 50 | 45 | |

**[L. 21, 26]**. These volumes were calculated using the following option: the volume of hole/peak in TalyMap software used for wear levels computation; ($V_{disc}$+) or ($V_{ball}$+) – volume of peak, while ($V_{disc}$-) or ($V_{ball}$-) – volume of hole.

The wear level of disc was assessed after surface levelling. Before calculating the wear of solid balls, the form was eliminated using a hollow sphere.

The chemical constitution of worn disc was also analysed using a scanning electron microscope equipped with an EDS analyser. Each tribological test was repeated at least two times.

## RESULTS AND DISCUSSION

**Table 2** presents specifications of surface topographies of machined disc samples. The following parameters are included in these tables: standard deviation of height Sq, the texture aspect ratio Str, autocorrelation length Sal, skewness Ssk, kurtosis Sku, and rms. slope Sdq **[L. 27]**. **Figure 1** and **Figure 2** present contour plots of disc samples.

From among disc surfaces (**Table 2** and **Figure 1**) samples after rough (VBI1) and finish vapour blasting (VBI2) have isotropic characters (the values of the Str parameter are between 0.86 and 0.87). The rms. slopes of these textures Sdq are the biggest. Anisotropic one-directional samples after finish milling (MI1 and MI3) and grinding (GI1 and GI2) were also tested. From among these textures, the MI3 specimen is characterised by the biggest height and autocorrelation length Sal. The standard deviations of roughness height and correlation length of a texture after finish grinding (GI1) are smaller than those of a surface after rough grinding (GI2). The height of a milled disc (MI1) is similar to the amplitudes of ground samples. The values of spatial parameter Sal of finish milled samples are larger than those of ground disc specimens. A disc after rough milling (MI2) is characterised by the largest height Sq and correlation length Sal from all samples studied in the tests I. The standard deviations of roughness height Sq of samples PI after polishing and LI after lapping are the smallest. Surfaces after milling have deterministic, but after grinding, vapour blasting, and lapping, the surfaces had random characteristics.

At the smaller frequency of oscillations (20 Hz), the mean value of the maximum coefficient of friction was assessed after eliminating initial results of tests (rapid increase of the friction coefficient probably due to surface roughness change and debris formation) between 50 and 900 seconds; however, the final coefficient of friction was evaluated by averaging its values obtained between 600 and 900 seconds. At the higher frequency (50 Hz), the average coefficient of friction was evaluated between 50 and 360 seconds, but the final evaluation was between 300 and 360 seconds.

The Hertzian contact pressures for a normal load of 45 N were 1652 MPa, while the elastic contact diameter was 0.228 mm (larger than the highest stroke of 0.2 mm).

Tests were characterised by a low variation of the friction coefficient. The scatter of the average coefficient of friction for the sliding pair with the same disc sample was typically smaller than 0.02. The scatter of the total wear of the tribological system was typically not higher than 10%.

It is evident that the wear of the ball was smaller than the wear of disc in most cases (except for the sliding pairs with the samples MI1, MI3 and GI2) in tests IA. The highest total wear was obtained for disc surfaces after rough milling MI2 and vapour blasting VBI1, while the smallest for the textures after finish milling MI1 and MI3. Comparatively high volumetric wear was observed for the friction pair with the smoothest surface after polishing PI. The highest average value of the coefficient of friction COF50-900 was obtained for disc surfaces after vapour blasting (VBI1) and lapping (LI), but the smallest was after rough grinding GI2 and especially finish milling (MI1 and MI3).

**Table 2. Surface texture parameters of machined discs**
Tabela 2. Parametry struktury geometrycznej powierzchni badanych dysków

| Surface | Parameters | | | | | |
|---|---|---|---|---|---|---|
| | Sq, μm | Ssk | Sku | Sal, mm | Str | Sdq |
| VBI1 | 2.91 | -0.4 | 4.4 | 0.0201 | 0.863 | 0.532 |
| VBI2 | 2.4 | -0.45 | 6.3 | 0.0201 | 0.87 | 0.452 |
| MI1 | 0.48 | 0.38 | 2.9 | 0.02 | 0.015 | 0.074 |
| MI2 | 6.8 | -0.7 | 4.6 | 0.231 | 0.164 | 0.25 |
| MI3 | 1.23 | -0.8 | 3.14 | 0.06 | 0.036 | 0.094 |
| GI1 | 0.36 | -0.36 | 3.3 | 0.008 | 0.02 | 0.1 |
| GI2 | 0.57 | -0.78 | 4.95 | 0.014 | 0.019 | 0.131 |
| PI | 0.00098 | -0.07 | 3.2 | 0.117 | 0.218 | 0.0029 |
| LI | 0.07 | -0.9 | 5.8 | 0.029 | 0.28 | 0.0207 |

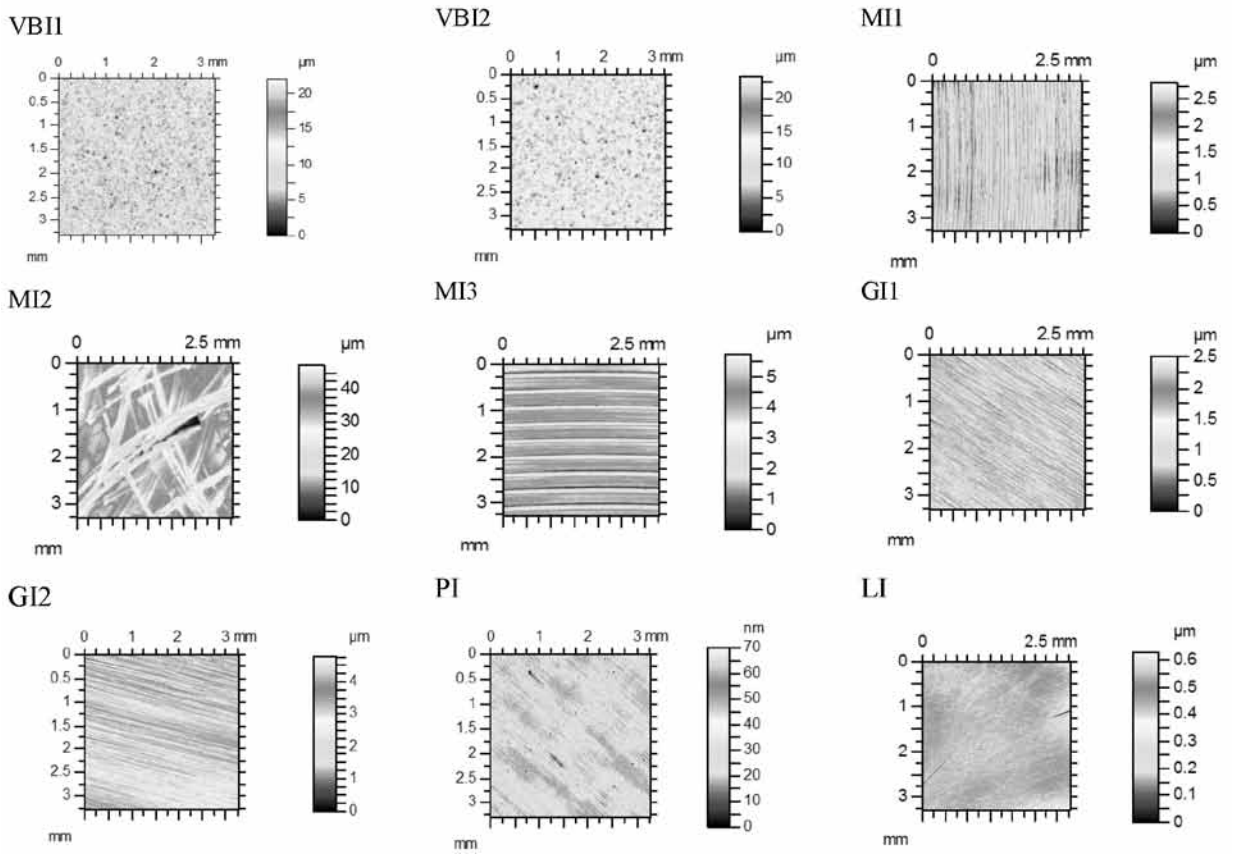


**Fig. 1. Contour plots of surface textures**
Rys. 1. Mapy konturowe powierzchni badanych dysków

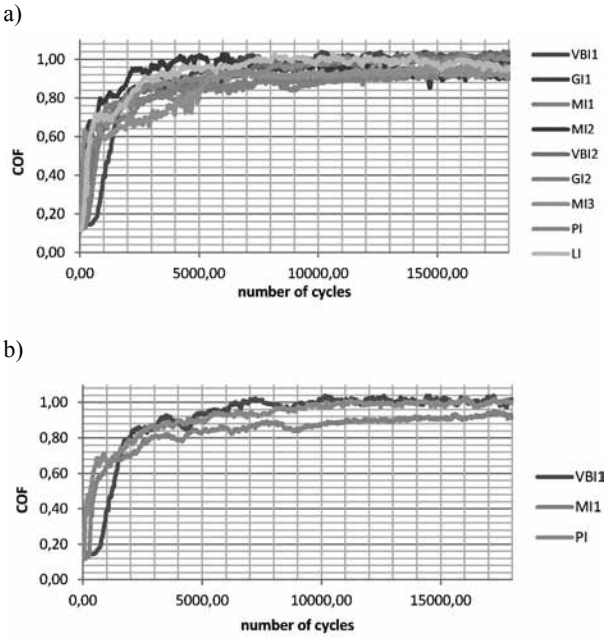


**Fig. 2. Maximum friction coefficient versus time in tests IA for sliding pairs with all (a) and selected (b) disc samples (A = 0.1 mm, P = 45 N, f = 20 Hz)**
Rys. 2. Wartość maksymalna współczynnika tarcia w funkcji czasu dla testu IA dla wszystkich (a) oraz wybranych (b) badanych par

**Figure 2** shows values of maximum friction coefficients versus time for sliding pairs with all and selected disc samples. The coefficients of friction, after initially increasing, obtained stable values after 5000–7000 cycles. In the initial parts of the tests, the sample MI2, after rough milling, led to the highest frictional resistance, but the sample after finish milling (MI1) to the lowest frictional resistance. In initial test portion, the relative differences between the coefficients of friction for various sliding pairs were the largest (up to 30%). From the analysis of **Figure 2b**, it is evident that the coefficient of friction of the assembly with the MI1 sample is smaller than those of the sliding pairs with the PI and VBI1 samples. The average coefficient of friction was proportional to the total wear of the tribologic system (**Figure 3a**) and wear of discs, but inversely proportional to wear of balls. The volumetric wear of discs was inversely proportional to the wear of balls (**Figure 3b**). When ball movement was parallel to the lay (main texture direction), the coefficient of friction was larger compared to sliding orthogonal to the lay (**Figure 4**).

**Figure 5** shows values of the maximum friction coefficient versus time for assemblies with all and selected disc samples in tests IB. The wear of the ball was higher than the wear of disc with two exceptions:

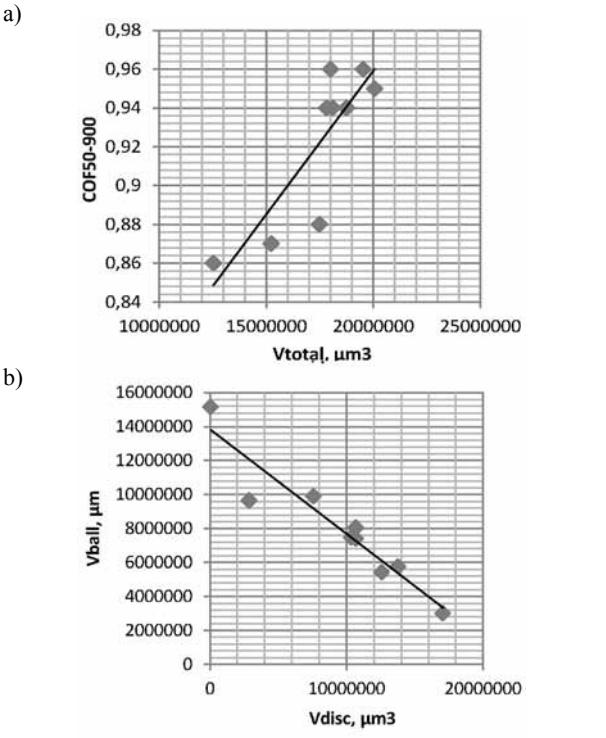


**Fig. 3. Average value of the coefficient of friction versus total volumetric wear of system (a), volumetric wear of discs versus volumetric wear of balls (b) in the tests IA (A = 0.1 mm, P = 45 N, f = 20 Hz)**

Rys. 3. Średnia wartość współczynnika tarcia w funkcji całkowitego zużycia objętościowego systemu (a), zużycie objętościowe dysków w funcji zużycia objetościowego kulek (b) dla testu IA (A = 0.1 mm, P = 45 N, f = 20 Hz)

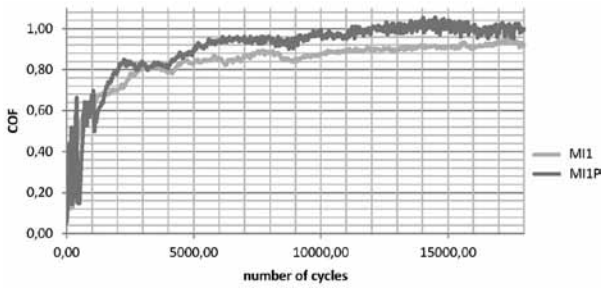


**Fig. 4. Maximum coefficient of friction versus time for sample MI1 for ball movement orthogonal and parallel (MI1P) to the lay in the tests IA (A = 0.1 mm, P = 45 N, f = 20 Hz)**

Rys. 4. Maksymalna wartość współczynnika tarcia w funkcji czasu dla próbki MI1 przy ruchu kulki prostopadłym i równoległym (MI1P) do kierunku tekstury dla testu IA (A = 0.1 mm, P = 45 N, f = 20 Hz)

the roughest specimens VBI1 and MI2. The highest total wear was obtained for the disc surfaces of the biggest amplitudes (VBI1 and MI2), while the smallest was for disc samples after finish milling (MI1 and MI3) as well as rough grinding (GI2). The smallest values

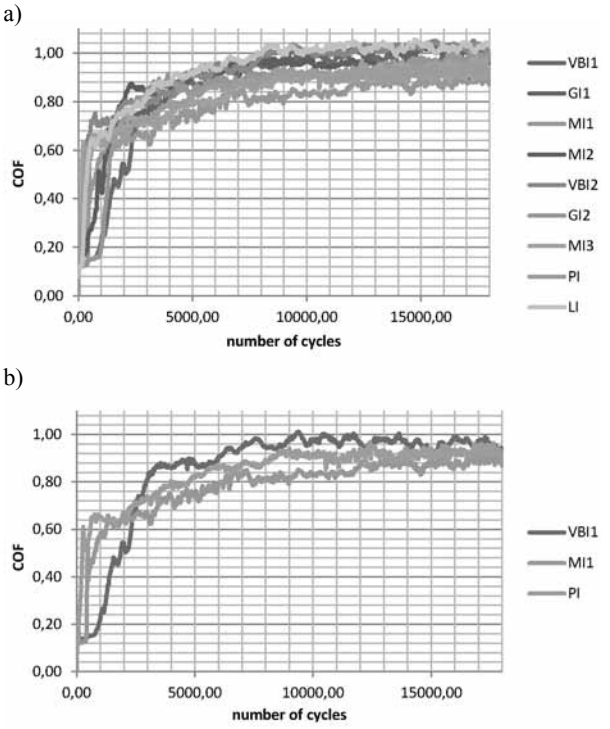


**Fig. 5. Maximum friction coefficient versus time in tests IB for sliding pairs with all (a) and selected (b) disc samples (A = 0.075 mm, P = 45 N, f = 20 Hz)**

Rys. 5. Maksymalna wartość współczynnika tarcia w funkcji czasu podczas testu IB dla wszystkich (a) oraz wybranych (b) par trących (A = 0.075 mm, P = 45 N, f = 20 Hz)

of the mean coefficient of friction COF50-900 were obtained for disc samples after finish milling (MI1 and MI3). Similarly to tests IA, the average coefficient of friction was proportional to the wear of the disc and inversely proportional to the wear of the ball. A decrease in the amplitude of oscillations from 0.1 to 0.075 mm caused a decrease in the mean coefficient of friction and had a marginal effect on the final coefficient of friction, while volumetric wear considerably decreased. The coefficient of friction obtained stable values after 9000 cycles, and the scatters of the coefficients of friction were similar in various test parts.

In Tests IC of the smallest stroke, the total wear of all the tested assemblies was similar, except for the assembly with the VBI1 disc sample of the biggest wear. For all sliding pairs, the wear of the disc was much smaller than the wear of the ball. Similar to the larger amplitude (Tests IA and IB), the wear of discs was inversely proportional to the wear of balls. The coefficient of friction was the smallest for the sliding pairs with the surfaces after finish milling (MI1 and MI3) followed by the assembly containing the surface after rough grinding (GI2). The mean coefficient of friction COF50-900 was proportional to the total wear

and the wear of discs but inversely proportional to wear of balls. No similar correlation was found for the final coefficient of friction COF600-900.

The coefficients of friction obtained stable values after approximately 12000 cycles (**Figure 6a**). A decrease in stroke from 0.15 to 0.1 mm caused marginal changes in the coefficient of friction and a considerable decrease in wear.

The Hertzian contact pressure for a normal load of 15 N was 1145 MPa, while the elastic contact diameter was 0.158 mm, which is higher than the stroke of 0.1 mm.

In Tests ID, in most cases, the wear of the ball was higher than the wear of the disc, and the roughest samples VBI1, MI2 were the exceptions. The highest total wear was obtained for the assembly with the roughest disc sample after rough milling (MI2). The volumetric wear of the other assemblies was similar. The smallest values of the mean coefficient of friction (COF50-900) were found for the sliding pairs with the samples after finish milling (MI1 and MI3). A decrease in normal load from 45 to 15 N caused an increase in the coefficient of friction and a reduction of total wear of the tribologic system. During Tests ID, the coefficient of friction increased, obtained a maximum value, and then decreased, which is different from results obtained in the other analysed tests. Therefore, the mean coefficients of friction (COF50-900) were higher or similar to the final friction coefficients (COF600-900). In initial parts of tests, the disc after vapour blasting (VBI1) gave a higher coefficient of friction compared to the samples MI1 and PI (**Figure 6b**).

In Tests IE, typically, except for the disc VBI1, the wear of the ball was much larger than of the disc. The highest total wear was obtained for the sliding pair with the roughest sample (MI2), which gave the highest coefficient if friction. Similarly to results of the other analysed tests, the wear of the balls was inversely proportional to the wear of the discs. Small values of the coefficient of friction were obtained for assemblies with the samples after finish milling (MI1 and MI3) as well as rough grinding (GI1). In test runs, the coefficients of friction increased and obtained stable values after 8000–9000 cycles, some fluctuations are visible for the test run with the MI1 disc (**Figure 7a**). In most cases, an increase in the frequency of oscillations (compared to tests ID) for the same number of cycles led to a decrease in total wear and an increase in the coefficient of friction.

In Tests IF, the wear of the balls were considerably higher than the wear of the discs. The smallest coefficients of frictions were obtained for assemblies with samples after milling (MI1 and MI3) followed by the disc after rough grinding (GI2). An increase in frequency in relation to Tests IC caused smaller total wear and a marginal change of the coefficient of friction. During tests, the coefficients of friction increased as the tests progressed (**Figure 7b**).

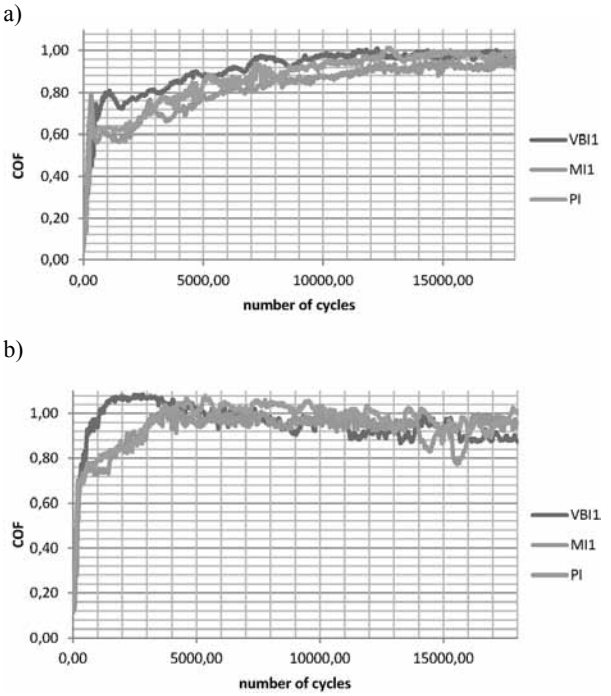


**Fig. 6. Maximum friction coefficient versus time for selected sliding pairs from in tests IC; A = 0.05 mm, P = 45 N, f = 20 Hz; (a) and in tests ID; A = 0.05 mm, P = 15 N, f = 20 Hz (b)**

Rys. 6. Maksymalna wartość współczynnika tarcia w funkcji czasu dla wybranych par trących podczas testu IC; A = 0,05 mm, P = 45 N, f = 20 Hz; (a) oraz w teście ID; A = 0,05 mm, P = 15 N, f = 20 Hz (b)

The shapes of fretting loops shown in **Figure 8** are typical for the gross slip regime. In various types of tests, the smallest values of the coefficient of friction were obtained for disc samples after finish milling (MI1 and MI2) followed by the sample after rough grinding (GI2). These surfaces are one-directional anisotropic textures. The low frictional resistance of sliding pairs with these samples is probably connected with the formation of the oxide layer. The position of the direction of sliding in relation to the lay (main surface direction) of the disc surface is of substantial importance. When ball movement was perpendicular to this lay, the coefficient of friction was smaller than that obtained for sliding along the lay (**Figure 4**). This tendency was more important for larger displacement amplitudes. Contrary to other textures, milled surfaces formed by cutting process of deterministic character had peaks milder than those formed by abrasive processes. Similar results were obtained during contact between a steel ball of 60 HRC hardness and a steel disc of 43 HRC hardness **[L. 28]**. Small coefficients of friction were connected with small wear levels of discs in tests IA, IB, IC, and ID. Better tribological performance of assembly with the ground GI2 disc than GI1 is probably caused by larger spatial parameter Sal of the GI2 disc. The largest total wear

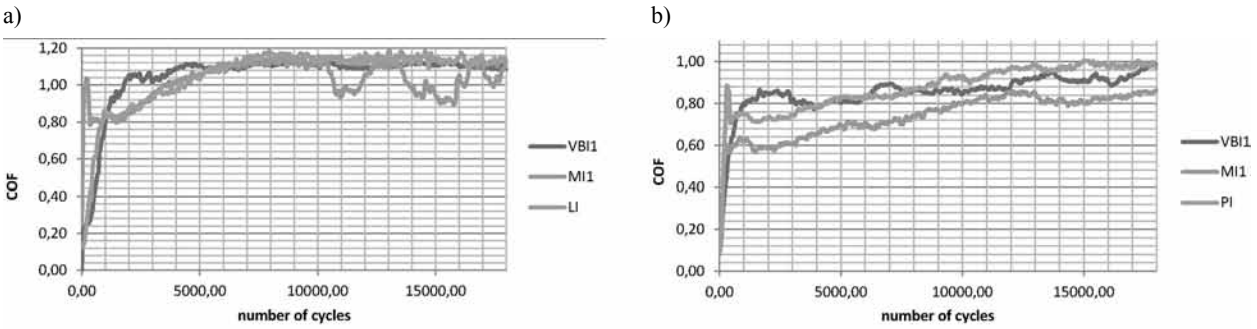


**Fig. 7. Maximum friction coefficient versus time for selected sliding pairs from in tests IE; A = 0.05 mm, P = 15 N, f = 50 Hz; (a) and in tests IF; A = 0.05 mm, P = 45 N, f = 50 Hz (b)**

Rys. 7. Maksymalna wartość współczynnika tarcia w funkcji czasu dla wybranych par trących podczas testu IE; A = 0,05 mm, P = 15 N, f = 50 Hz; (a) oraz w teście IF; A = 0,05 mm, P = 45 N, f = 50 Hz (b)

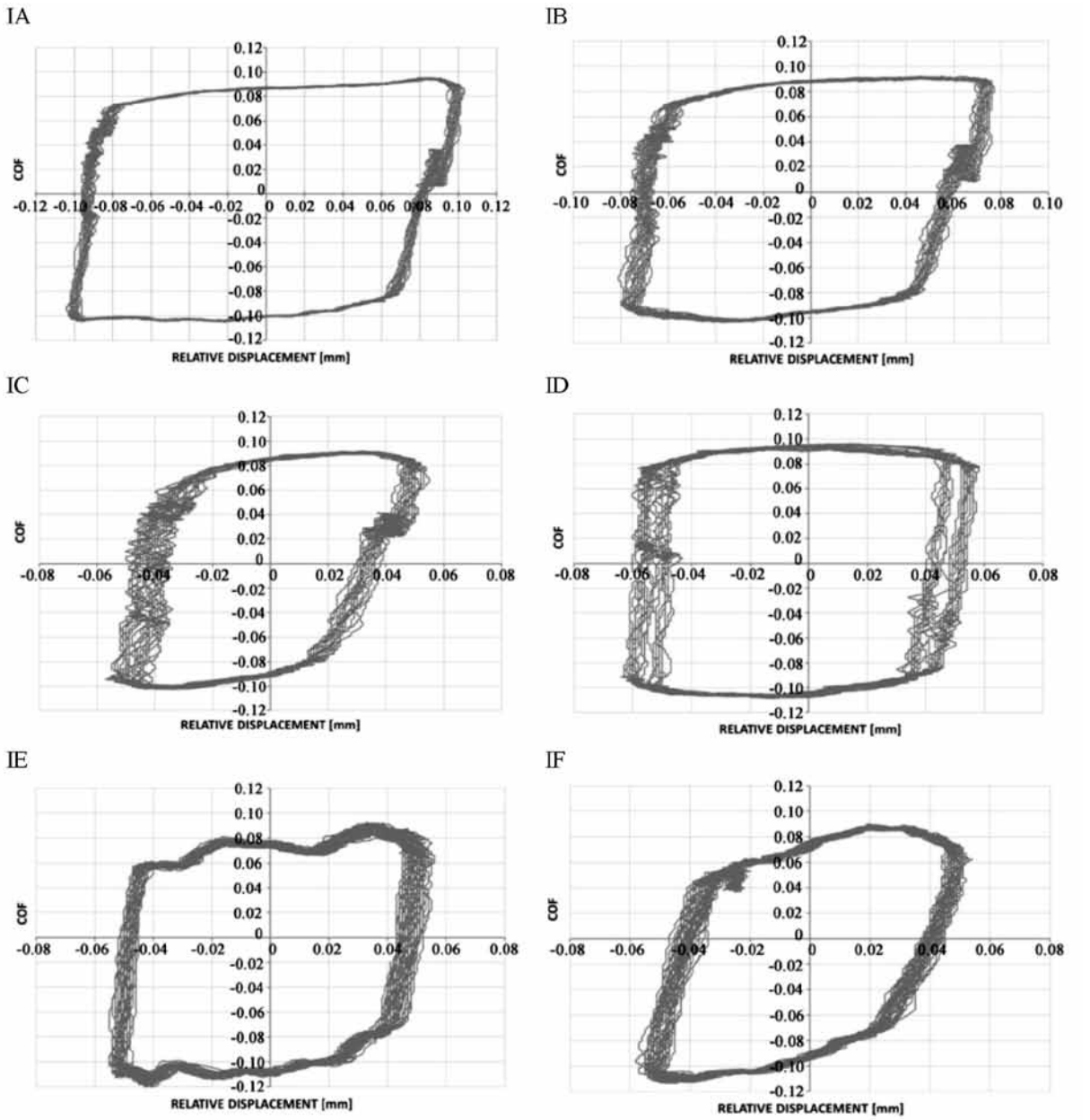


**Fig. 8. Fretting loops for assembly with PI disc after various types of tests**

Rys. 8. Pętle frettingowe dla skojarzeń zawierających tarczę PI po różnych wariantach testów

corresponded to the highest roughness of discs MI2 in tests IA, IB, ID, and IE. The disc sample after vapour blasting (VBI1) led to a typically high coefficient of friction and high wear of disc but a small wear of balls. After comparing **Figure 9** and **Figure 10**, it is evident that the wear level of the MI1 disc was smaller but that of the co-acted ball was higher than those of the assembly containing the VBI1 disc. The wear of the disc was higher than measured, because the wear scars were occupied by a compacted debris layer. Loose debris on the disc specimen was removed, but compressed and adhered oxidised debris embedded into the softer disc surface remained. After the examinations of the bottoms of wear tracks using scanning electron microscopy equipped with an EDS function, the presence of oxygen was found; about 30%, see **Figure 11**. Typically (except for Tests IA) that of the ball was higher than that of the disc. Oxidised debris of high hardness embedded into the softer disc material caused high wear of balls. Build-ups with compacted debris were formed inside the disc scars, which is connected with higher wear of balls in corresponding places. These build-ups can be seen in **Figure 9**. The oxygen content in the place of the presence of build-ups (point 3 in **Figure 11**) is smaller

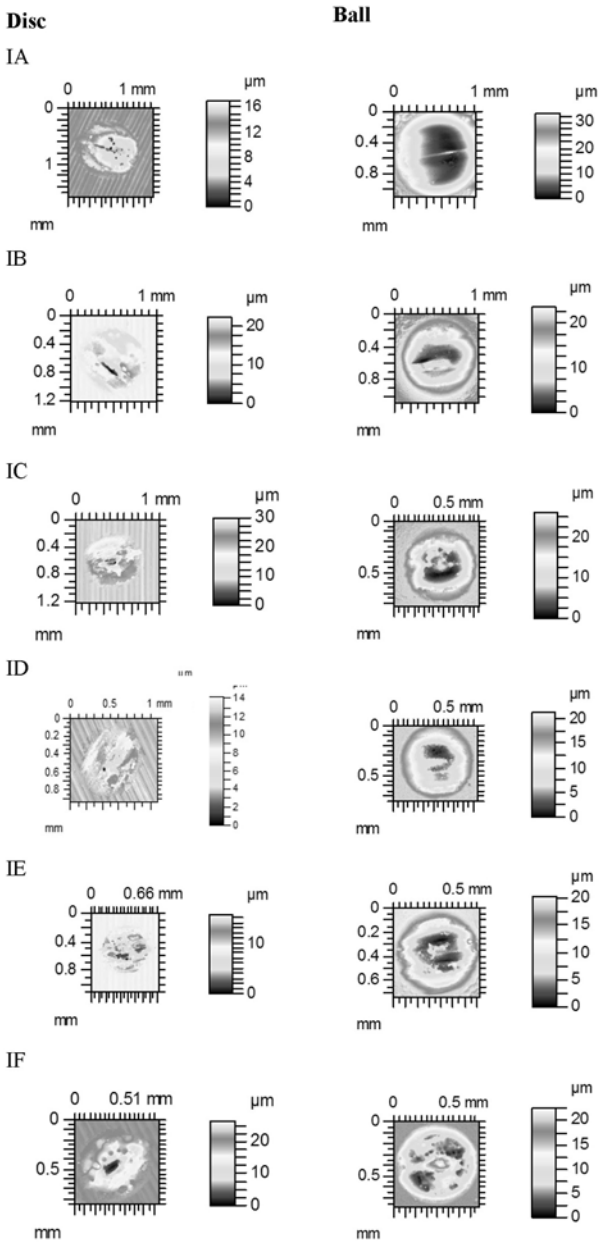


**Fig. 9. Contour plots of disc MI1 and co-acted balls after tests**

Rys. 9. Mapy powierzchni dysku MI1 i współpracujących kulek po badaniach

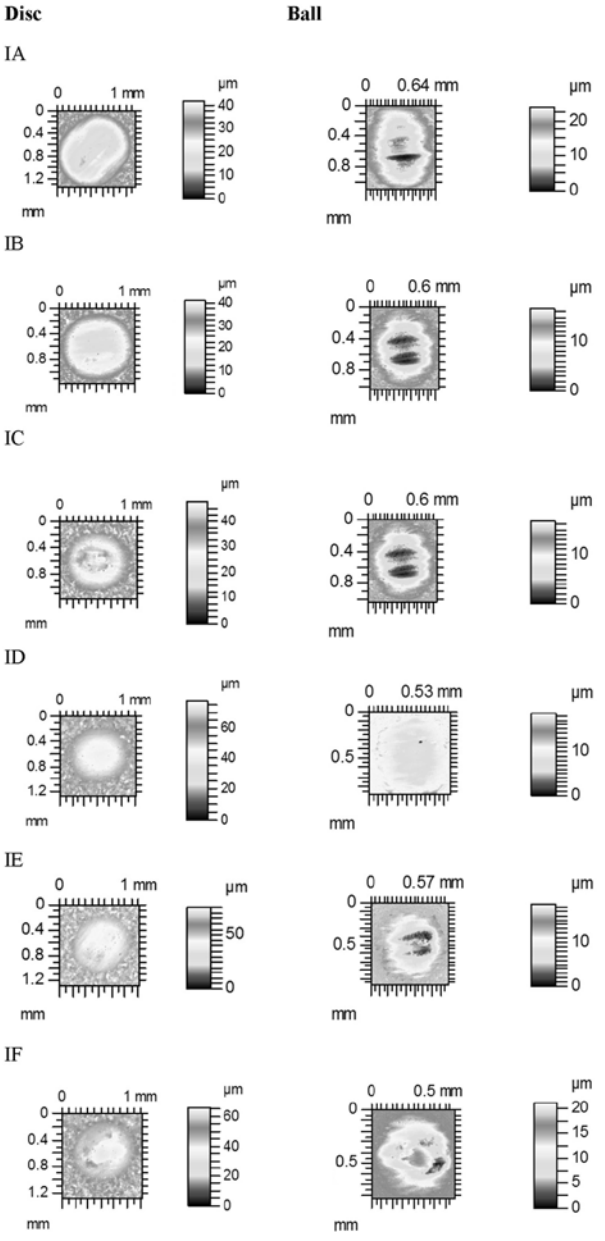


**Fig. 10. Contour plots of disc VBI1 and co-acted balls after tests**

Rys. 10. Mapy powierzchni dysku VBI1 i współpracujących kulek po badaniach

than in the bottom of wear tracks – about 20%. The contents of iron and oxygen inside the wear track were uniform – see **Figure 12**.

A decrease in the normal load caused an increase in the coefficient of friction and a decrease in wear. Due to a decrease in stroke, for the same normal load, wear decreased, and the friction force later achieved the stable value, while changes of the final coefficient of friction were marginal. An increase in frequency from 20 Hz to 50 Hz caused a reduction of wear and an increase in the coefficient of friction for smaller normal load (15 N).

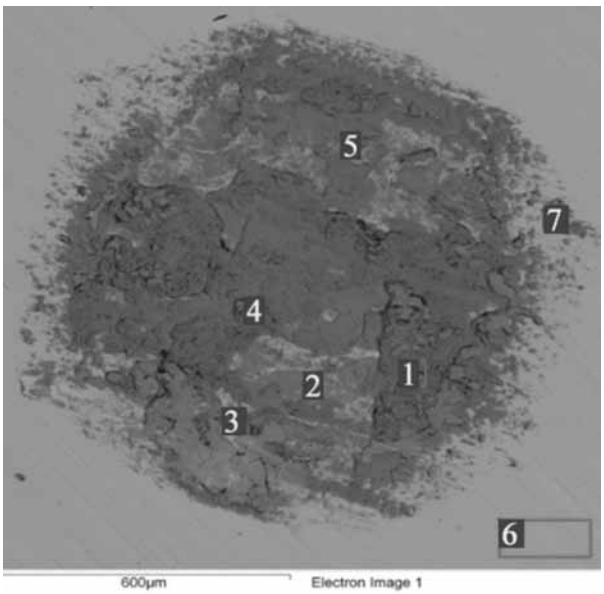


| Spectrum | O | Si | Cr | Mn | Fe |
|---|---|---|---|---|---|
| 1 | 31.26 | 0.40 | 0.92 | | 53.99 |
| 2 | 23.15 | 0.23 | 0.87 | 0.33 | 69.03 |
| 3 | 18.86 | 0.26 | 0.90 | 0.39 | 75.19 |
| 4 | 30.96 | 0.75 | 0.69 | | 37.65 |
| 5 | 28.05 | 0.48 | 0.90 | | 57.54 |
| 6 | | 0.28 | 1.01 | 0.50 | 95.44 |
| 7 | 15.91 | 0.28 | 0.83 | 0.50 | 74.62 |

**Fig. 11. The results of chemical constitution of worn disc PI after tests IB**

Rys. 11. Wyniki składu chemicznego zużytego dysku PI po badaniach IB

a)

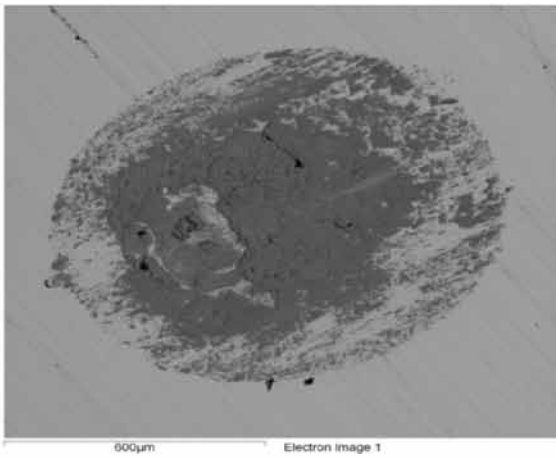


b)

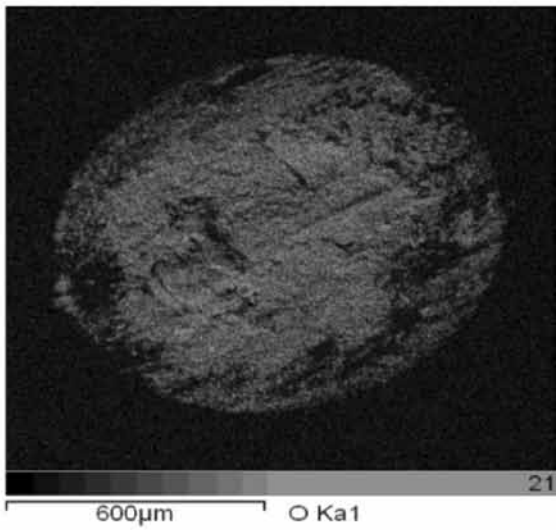


c)

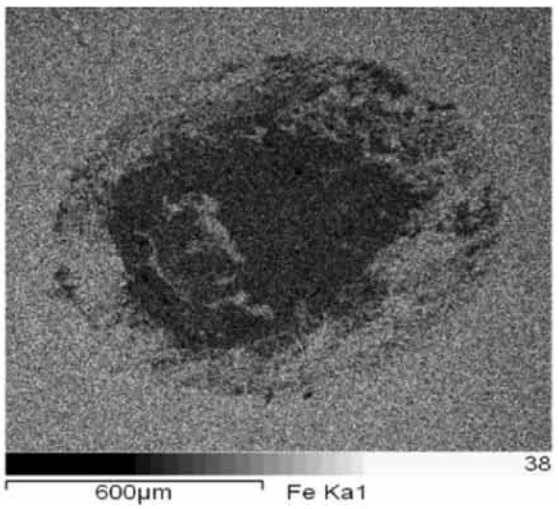


**Fig. 12. View of sample LI after tests IB (a), mapping of content of oxygen (b) and iron (c)**

Rys. 12. Widok próbki LI po badaniach IB (a), mapping zawartości tlenu (b) i żelaza (c)

## CONCLUSIONS

Surface texture has a significant effect on the coefficient of friction. The smallest coefficients of friction were achieved for deterministic one-directional milled surfaces, when ball movement was perpendicular to the main disc texture direction. The coefficient of friction was typically proportional to the volumetric wear of the tribological system. The wear of discs was smaller than the wear of balls, which was caused by debris embedding into the softer disc surface. The wear of balls was inversely proportional to the wear of discs. The largest total wear corresponded to the highest roughness of discs. Due to a stroke decrease, for the same normal load, the friction force later achieved a stable value.

A decrease in stroke caused a decrease in wear but has a negligible effect on the friction force. A normal force decrease led to a larger coefficient of friction and a smaller volumetric wear of the tribological system. An increase in frequency caused a decrease in wear and an increase in the coefficient of friction for the smaller normal load of 15 N.

## REFERENCES


1. Fouvry S., Kapsa Ph., Vincent L.: Analysis of sliding behavior for fretting loading: Determination of transition criteria, Wear 185 (1995) 21–46.
2. Vingsbo O., Soerberg S.: On fretting maps, Wear 126 (1988) 131–147.
3. Zhou Z.R., Nakazawa S., Zhu M.H., Maruyama N., Kapsa Ph., Vincent L.: Progress in fretting maps. Tribology International 39 (2006) 1068–1073.
4. Varenberg M., Etsion I., Halperin G.: Slip index: a new unified approach to fretting, Tribology Letters 17 (2004) 569–573.
5. Varenberg M., Etsion I., Altus E.: Theoretical substantiation of the slip index approach to fretting, Tribology Letters 19 (2005) 263–264
6. Fouvry S., Paulin C., Liskiewicz T.: Application of an energy wear approach to quantify fretting contact durabiliy: Introduction of a wear energy capacity concept, Tribology International 40 (2007) 1428–1440.
7. Varenberg M., Halperin G., Etsion I.: Different aspects of the role of wear debris in fretting wear. Wear 252 (2002) 902–910.
8. Ding J., McColl I.R., Leen S.B., Shipway P.H.: A finite element based approach to simulating the effects of debris on fretting wear, Wear 26 (2007) 481–491.
9. Iwabuchi A.: The role of oxide particles in the fretting wear of mild steel, Wear 151 (1991) 337–344.
10. Diomidis N., Mischler S.: Third body effects on friction and wear during fretting of steel contacts, Tribology International 44 (2011) 1452–1460.
11. Hu Q., McColl I.R., Harris S.J., Waterhouse R.B.: The role of debris in the fretting wear of a SiC reinforced aluminium alloy matrix composite, Wear 245 (2000) 10–21.
12. Berthier Y., Vincent L., Godet M.: Fretting fatigue and fretting wear, Tribology International 22 (1989) 235–242.
13. Lemm J.D., Warmuth A.R., Pearson S.R, Shipway P.H.: The influence of surface hardness on the fretting wear of steel pairs – Its role in debris retention in the contac, Tribology International 81 (2015) 258–266.
14. Ohmae N., Tsukizoe T.: The effect of slip amplitude on fretting, Wear 27 (1974) 281–294.
15. Li J., Lu Y.H.: Effects of displacement amplitude on fretting wear behaviors and mechanism of Inconel 600 Alloy. Wear 304 (2013) 223–230.
16. Toth L.: The investigation of the steady stage of steel fretting, Wear 20 (1972) 277–286.
17. Soderberg S., Bryggman U., McCullough T.: Frequency effects in fretting wear, Wear 110 (1986) 19–34.
18. Kayanba T., Iwabuchi A.: Effect of hardness of hardened steel and the action of oxides on fretting wear, Wear 66 (1981) 27–41.
19. Ramesh R., Gnanamoorthy R.: Effect of hardness on fretting wear behavior of structural steel En 24, against bearing steel, En 31. Materials Design 28 (2007) 1447–1452.
20. Budinsky K.C., Effect of hardness differential on metal-to-metal fretting damage, Wear 301 (2013) 501–507.
21. Lemm J.D., Warmuth A.R., Pearson S.R., Shipway P.H.: The influence of surface hardness on the fretting wear of steel pairs – its role in debris retention in contact, Tribology International 81 (2015) 258–266.
22. Kubiak K.J., Liskiewicz T.E., Mathia T.G.: Surface morphology in engineering applications: Influence of roughness on sliding and wear in dry fretting, Tribology International 44 (2011) 1427–1432.
23. Kubiak K.J., Bigerelle M., Mathia T.G., d'Hardivilliers W.: Roughness of interface in dry contact under fretting conditions, Proceedings on the 13th International Conference on Metrology and Properties of Engineering Surfaces, 12–15 April 2011, Twickenham Stadium, UK, 99–102.
24. Pawlus P., Michalczewski R., Dzierwa A., Lenart A.: The effect of random surface topography height on fretting in dry gross slip conditions, Proceedings of the Institution of Mechanical Engineers, part J: Journal of Engineering Tribology 228 (2014) 1374–1391.
25. Yoon Y., Etsion I., Talke F.E., The evolution of fretting wear in a micro-spherical contact, Wear 270 (2011) 567–575.
26. Elleuch K., Fouvry S.: Wear analysis of A357 aluminum alloy under fretting, Wear 253 (2002) 662–672.
27. Leach R. (Ed.) Characterisation of areal surface texture. Springer-Verlag Berlin, Heidelberg 2013.
28. Lenart A., Pawlus P., Dzierwa A., Sep J.: The effect of surface topography on dry fretting in the gross slip regime. Archives of Civil and Mechanical Engineering 17 (4) (2017) 894–904.